Characterization of Atmospheric Pressure Microplasma Jet Source and its Application to Bacterial Inactivation

Sun Ja Kim, Tae Hun Chung,* Se Hwan Bae, Sun Hee Leem

Atmospheric pressure microplasma jet sources driven by radio-frequency wave of 13.56 MHz and by low frequency continuous wave of several kHz ac were fabricated and characterized. The source consists of an ac-driven copper wire (needle) surrounded by dielectric layer that are placed in a glass tube, and a ground plane electrode (pin-to-plane electrode configuration). The basic physical and chemical properties of the plasma jet sources, such as optical emission spectrum, gas temperature, and power deposition were investigated. With various geometrical and operational parameters changed, plasma jets showed different discharge characteristics. The geometrical parameters include the length of the pin wire exposed to the plasma, the distance between the pin to the outlet of the glass tube, and the distance between the pin and the plane electrode. The operational parameters include the applied voltage (amplitude and frequency) and the gas flow rate. As an example of biomedical application of the microplasma jets, the bacterial inactivation experiment was performed. Plasma power (or applied voltage), treatment time, and needle-to-sample distance were varied and the bacterial inactivation effects of these parameters were observed.

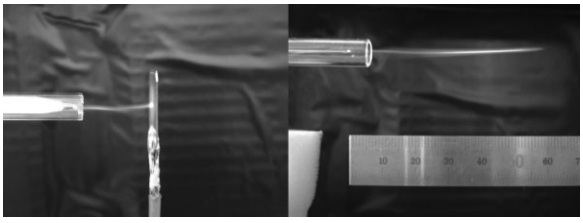

Introduction

Non-thermal plasmas offer high excitation selectivity and energy efficiency in plasma chemical reactions. They are sources of UV, Visible and IR radiation, free radicals and active species that can play important roles in various techniques. Non-thermal atmospheric discharges and their applications in biomedical treatments have become hot issues of current low-temperature plasma research.[1–4] Atmospheric pressure microplasma jet sources are among the most plausible candidates for that purpose. They have been operated at an excitation frequency either in the several tens of kilohertz ac range (or pulsed mode) or in the radio-frequency (RF) range.[5–8] Due to various design configurations and operation conditions of microplasma jets, the factors governing the discharges, for instance, heat, charged particle, electric field, chemically active species may be very distinct.[9] Atmospheric pressure glow

S. J. Kim, T. H. Chung, S. H. Bae
Department of Physics, Dong-A University, Busan 604-714, Republic of Korea
E-mail: thchung@dau.ac.kr
S. H. Leem
Department of Biological Science, Dong-A University, Busan 604-714, Republic of Korea

Plasma Process. Polym. **2009**, *6*, 676–685

DOI: 10.1002/ppap.200850001

discharges have been shown to inactivate many different microorganisms, including bacteria,[10–12] fungus,[13] bacterial spores,[14–16] plant cells,[8] cancer cells,[3] proteinaceous matters,[17,18] and even genetic DNA.[9] Different designs have been investigated for prospective use in biomedical applications. For biomedical applications, the plasma sources have to provide truly non-thermal plasmas near room temperature without any electrical and chemical risks. In order to treat living tissues, the plasma should guarantee the low current and low gas temperature. For better control of the treatment processes, it is essential to understand the basic physical and chemical properties of the microplasma jets, such as electrical characteristics and power deposition, optical emission spectrum, and gas temperature.

In this paper, specially designed microplasma jet sources driven by a several tens of kilohertz ac and 13.56 MHz RF voltages are reported. The plasma generation in microplasma jets relies on various mechanisms: capactively coupled RF discharges, corona discharges, and dielectric barrier discharges (DBD).[19–22] A corona discharge appears as a luminous glow localized in space around a point tip (or wire) in a highly non-uniform electric field. Dielectric barrier discharges operating at atmospheric pressure are driven by a pulsed or sinusoidal voltage at frequencies from 50 Hz up to several tens of kHz (even up to RF) and at least one of electrodes has insulating layer. The dielectric barrier discharge in some cases has a safer feature of the source to prevent destruction in the case of an accidental arc formation. Some RF jet sources do not rely on the use of a dielectric barrier for their mode of operation.[23] The kHz sources instead rely on the presence of a dielectric barrier. The corona and DBD hybrid discharge systems are accessible to generate a glow discharge, and its characteristics can be controlled to suitable condition.[24] The devices developed here also utilize the combined working principles of capactively coupled RF discharge, corona discharge, and DBD. For both electrical discharges, the electrical circuit features are discussed and the characterization of the emission spectra is presented. The effects of various design configurations and operation parameters on the discharge properties of plasma are investigated. The effect of a ground plane electrode is also explored. As an example of biomedical application of the microplasma jets, the bacterial inactivation experiment was performed. In this work, a living tissue itself is used as one of the electrodes and directly participates in the active plasma discharge process. In biomedical applications, the counter electrode might be the patient or the medical instruments to be sterilized. If the medical instruments are made from polymers, the counter electrode concept will not work. Much can be learnt of the bactericidal capability and related physical mechanisms of low-temperature plasmas. Plasma power (or applied voltage), treatment time, and needle-to-sample distance were varied. And the bacterial inactivation effects of these parameters were observed. It is reasonable to assume that similar effects can be obtained on other microbes and cancer cells.

Experimental Part

Figure 1 depicts a scheme of two microplasma jet sources operating at atmospheric pressure. They consist of a plasma generator and the instruments used for measuring the voltage and current, and for detecting the optical emission intensity from the plasma. Figure 1a shows the jet source driven by several tens of kilohertz ac voltage. At the center of the glass tube there is a copper wire with a diameter of 0.9 mm and a pencil-shaped tapered end. The power source (FTLab HPSI200) of several tens of kilohertz is connected to the copper wire. The wire was concentric with a T-shaped cylindrical glass tube, which has an inside diameter of 6 mm and an outside diameter of 8 mm. The wire shaft was covered with a polyethylene insulator tube, leaving a length of 4 mm of the wire exposed to gas. The glass tube is filled with helium gas (99.999%) delivered at a flow rate in the range of 0.5–8 $l \cdot min^{-1}$, controlled by a flow meter (Kofloc RK1600R). The grounded plane electrode made of iron, with $2.5 \times 2.5\ cm^2$ in dimension and 0.5 mm in thickness, can be placed near the outlet of the glass tube. Figure 1b shows the jet source driven by 13.56 MHz RF voltage. The power is supplied by RF power generator (YS E03F) operating at 13.56 MHz and is connected to the tungsten wire through a homemade L-type matching network. The plasma generator consists of a tungsten wire (0.3 mm diameter) with a sharpened tip, confined in a Perspex tube with inner diameter of 7 mm and outer diameter of 10 mm. The wire was inserted coaxially in a Perspex tube and it protruded from the stainless steel holder by 1.3 cm. The RF plasma jet device utilizes a combination of a single pin corona discharge with an RF coaxial cylindrical capacitive discharge.[7] The incident and reflected power were monitored using a power meter (DAIWA DP810) connected via dual directional coupler (AR DC2600). In both cases, a and b, the

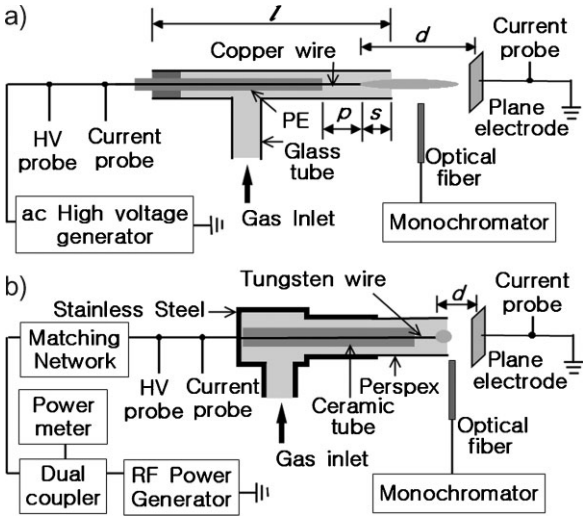

Figure 1. Schematic of the experimental setup. a) LF microplasma jet and b) RF microplasma jet with diagnostics systems.

waveforms of the voltage and the current were measured using a real time digital oscilloscope (LeCroy WS44Xs) via high voltage probe (Tektronix P5100) and current probe (Pearson 3972). To identify the reactive species that are generated in the discharge and subsequently expelled with the gas flow, spectra were recorded for the emission along the axis of the jet in the range from 200 to 800 nm. The light emitted by the microplasma was focused by means of optical fiber into entrance slit of 0.75 m monochromator (SPEX 1702), equipped with a grating of 1 200 grooves mm^{-1} and slit width of 100 μm. The light was collimated at the exit slit where a photomultiplier tube converted photons into an electric signal.

As an example of biomedical application of the microplasma jets, the bacterial inactivation experiment was performed. Escherichia coli (K-12 DH10B, competent cells) are inoculated from a glycerol stock into Luria–Bertani medium, the mixture is shaken for 14 h. The culture is grown at 37 °C with shaking. The E. coli (yielded final concentrations of about 3×10^6 CFUs $\cdot \mu l^{-1}$) suspension samples of 1 μl was deposited on the cover glass and directly exposed to the plasma. The distances of 2, 5 mm (the RF jet), and 1.5 cm (the LF jet) were chosen to place the samples from the tip of the pin electrode for exposure. The exposure time varied from 5 to 60 s with a 5 s step interval and the gas flow rate was kept constant ($1\,l \cdot min^{-1}$ for the RF jet, $2\,l \cdot min^{-1}$ for the LF jet). Following the standard microbiology procedure, for each experimental condition, five samples were prepared, three submitted to the plasma flowing afterglow, and one stored in the lab atmosphere for the same duration, as a control. Another control experiment was performed with the same gas flow, except with the plasma turned off. For the treated sample with the gas flow only, the same result was obtained as that for the control sample. The treated samples were then placed in a 10 ml of sterile distilled water and were thoroughly detached from the cover glass by using vortex and a repeated pipetting. The mixtures were serially diluted from 10^{-2} to 10^{-4}. Afterwards, the diluted solution were spread onto Petri dishes with the culture media (LB agar, Miller) and incubated at 37 °C for 20 h. After the incubation, the resulting colony forming units (CFU) were counted. Plasma power (or applied voltage), treatment time, and needle-to-sample distance were varied and the bacterial inactivation effects of these parameters were observed.

Results and Discussion

Low-frequency Microplasma Jet

Pin-to-plane electrode configuration is appropriate for certain applications, such as local and small-area surface treatments. When various geometrical and operational parameters changed, plasma jets showed different discharge characteristics. The geometrical parameters include the length of the pin wire exposed to the plasma (p), the distance between the pin to the outlet of the glass tube (s), and the distance between the pin and the plane electrode (d). The operational parameters include the applied voltage (amplitude and frequency) and the gas flow rate. When helium is injected from the gas inlet and 50 kHz sinusoidal 1.5 kV voltage is applied to the electrode in Figure 1a, a homogeneous plasma is generated and is launched through the end of the tube and in the surrounding air. The plasma has a cylindrical shape. The length of the plasma plume can be adjusted by the gas flow rate and the applied voltage. The length is indicative of the distance many reactive species can extend into the ambient atmosphere. The length of the plasma plume is shown as a function of applied voltage for two gas flow rates of $4\,l \cdot min^{-1}$ and $8\,l \cdot min^{-1}$ in Figure 2a. The plasma length increases with increasing the applied voltage. Since it is mainly the electrons that play an important role in the plasma generation, the electron oscillatory displacement is related to the plasma length.[7] Usually, the increasing of the helium feeding results in jet elongation, while further increase (here, up to $8\,l \cdot min^{-1}$) in the flow rate caused jet shortening and appearance of a turbulent tail at the jet's end. Larger gas flow rate seems to be equivalent to larger gas pressure. The electron oscillatory displacement is inversely proportional to the collision frequency, therefore, the plasma length decreases with increasing the gas flow rate. Since the electron displacement is proportional to the electric field, the plasma length increases with increasing the applied voltage. If the length of the pin wire electrode exposed to gas (p) is increased to 3.0 cm, the length of the plasma plume reaches up to 6 cm. The length of the plasma plume is correlated to the distance that reactive species travel into the ambient. Since at atmospheric pressure the recombination rate is so high, any real transport of reactive species from the plasma source over several centimeters will not work quantitatively. It is more likely that the excitation is due to an ionization wave along the gas channel and is triggered by the kHz excitation inside the source. This excitation might cause local dissociation of the source gas along that gas channel. Figure 2b shows current-voltage curves for two different p. The applied voltage is in the range of 800–1 700 V_{rms} and the measured total current is 3–7 mA_{rms}. It is observed that the case of $p = 3$ cm has a lower total current whereas it has a longer plume. The total current versus the applied voltage for the three different cases (one without the metal plane electrode, and others with the plane electrode of distances from the pin, $d = 1.5$ cm, and $d = 2.5$ cm) are presented in Figure 2c. The presence of the conducting plate enhances the total current. The case of small d has a higher current. The total current versus the applied voltage for different distances between the pin to the outlet of the glass tube (s) are presented in Figure 2d where they are also compared with the current for the case of different glass tube length (l). Although the length of glass tube itself contributes to a larger total current, the distance between the pin to the outlet of the glass tube (s) does not make significant effect on the total current. Figure 2e shows the frequency dependence of the total current of the low frequency (LF) plasma jet operating at 1400 V_{rms} and the gas flow rate of $3\ l \cdot min^{-1}$. From 30 kHz to 70 kHz, the total current

DOI: 10.1002/ppap.200850001

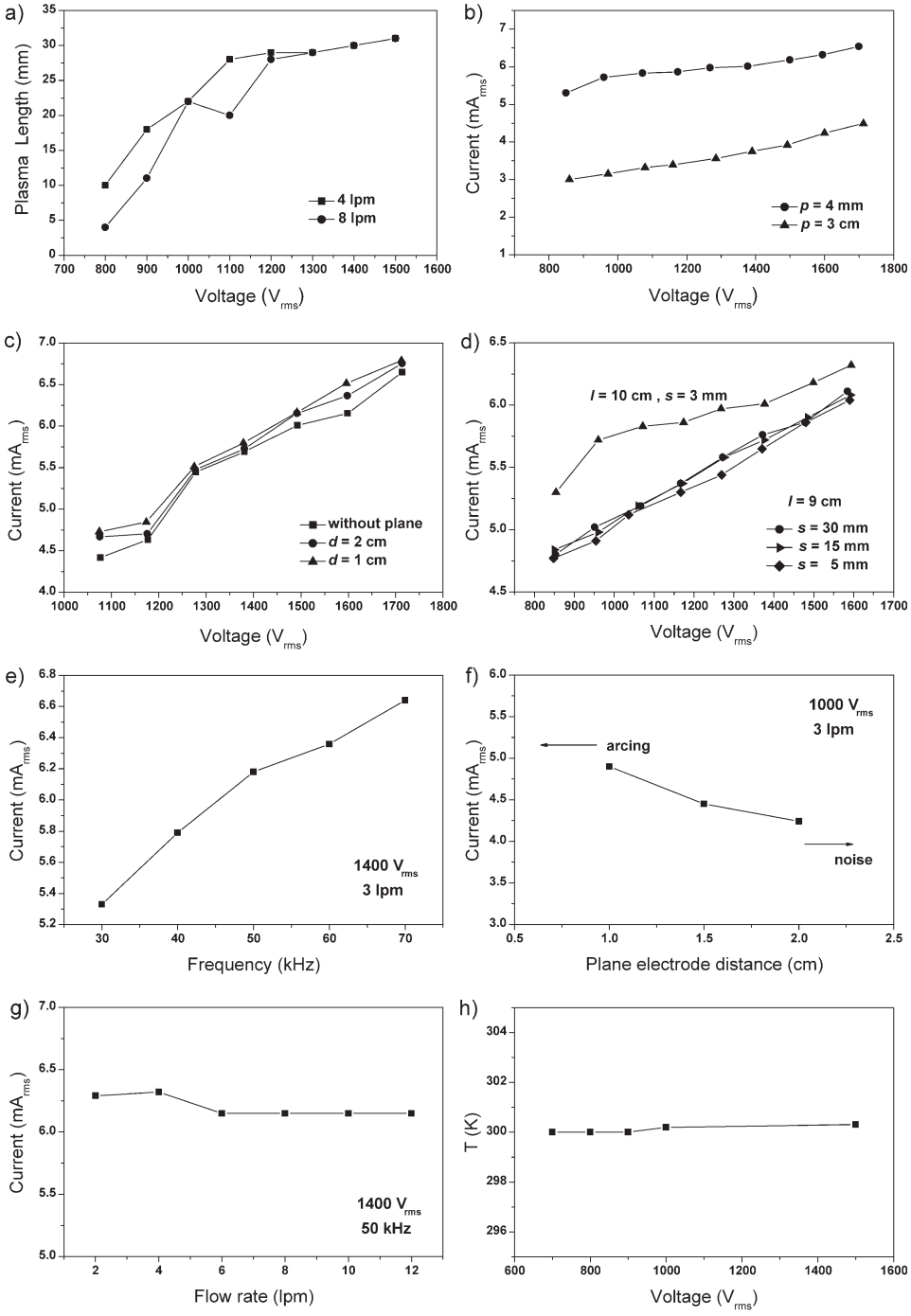

Figure 2. a) Plasma length as a function of applied voltage. b) Total current of the LF plasma jet as a function of applied voltage for two different *p*. c) Total current as a function of applied voltage for the cases of no metal plane and of the plane with two different *d* at the frequency of 50 kHz and the gas flow rate of 3 $l \cdot min^{-1}$. d) Total current vs. applied voltage for different geometrical parameters. e) The frequency dependence of the total current at the applied voltage of 1400 V and the gas flow rate of 3 $l \cdot min^{-1}$. f) Current collected at the ground plane electrode as a function of the distance of the plane electrode from the pin (*d*). g) Total current as a function of gas flow rate at the frequency of 50 kHz and the applied voltage of 1400 V. h) The measured gas temperature as a function of applied voltage for LF plasma jet.

increases from 5.3 to 6.7 mA_{rms}, suggesting more powerful plasma jets at higher frequencies. In order to maintain a suitable level of the reactive plasma species, the discharge current should not be small. A key issue for atmospheric-pressure microplasma jets is to expand their stability range to larger discharge currents with improved plasma reactivity. Figure 2f shows the variation of the current collected at the ground plane electrode with the distance of the plane electrode from the pin. It is observed that the current is decreased with increasing the distance exhibiting the characteristics of corona discharge. For the spacing closer than 1.0 cm, arcing is generated. For the spacing larger than 2.0 cm, the current monitor is plagued with noise. The influence of the gas flow rate on the total current is also shown in Figure 2g. The gas flow rate does not make a noticeable difference on the total current. Gas temperature is an important parameter in plasma application. Cold plasma jet provides a non-destructive tool to heat sensitive materials. As shown in Figure 2h, the gas temperature of the LF plasma was as low as the room temperature. The gas temperature was measured by using a fiber optic temperature sensor (FISO UM14&FOTL-L). The increase rate of the gas temperature with applied voltage in LF plasma is lower than that in the RF plasma (Figure 5c). Figure 3 shows the emission spectrum observed in the LF plasma (1 400 V_{rms}, 2 $l \cdot min^{-1}$). It shows that there were strong nitrogen molecular lines, as well as a few helium and oxygen atomic lines.[25–27] The strongest emission is the N_2^* line at 337.2 nm, and many nitrogen lines, excited He atom line at 706.5 nm, and excited oxygen line at 777 nm are shown. Oxygen and nitrogen species appear because the plasma was ejected into the ambient air where its energetic electrons and metastables ionized and excited air molecules. Atomic oxygen is usually generated by a dissociative collision between an oxygen molecule and an electron.

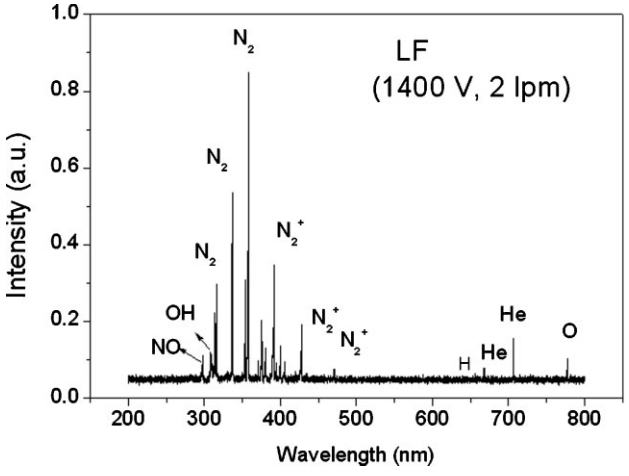

Figure 3. Emission spectrum from 200 nm to 800 nm observed in LF plasma jet (1 400 V_{rms}, 2 $l \cdot min^{-1}$).

Active species generated in the microplasma carry enough energy to remain active in spite of their transference to the free environment. The excited He is capable of exciting and ionizing a considerable amount of nitrogen molecules taking into account air molecule composition.[28] The LF plasma emission spectrum clearly indicates that OH and NO exist in the plasma plume.[3,5] The emission line at 656 nm corresponds to the H_α line, which is generated by the collision between water vapor molecule and electrons ($H_2O + e \rightarrow H + OH + e$). The emission intensity of OH at 309 nm is stronger than that of H_α at 656 nm. This indicates that OH radicals are also formed by the reaction of excited O with water vapor molecule ($H_2O + O \rightarrow 2\ OH$).[3] The NO serves a multitude of essential biological functions, including the bactericidal effect and the induction of the phagocytosis of bacteria and necrotic detrite.[29] These highly reactive species are considered to be most effective agents in attacking cells or organic material in general.

Radio-frequency Microplasma Jet

The RF plasma jet was powered at a frequency of 13.56 MHz. The supplied power varied from 5 to 10 W. The RF plasma was of spherical shape. Its length did not increase much with increasing the RF power. As shown in Figure 4, the corresponding amplitudes of the RF voltage ranged from 182 to 250 V_{rms} and the measured total current was 280–423 mA_{rms}. As the RF voltage is increased, the total current increases. This is a typical property of abnormal glow discharges. In ac driven plasmas with a given power, as driving frequency increases, the discharge voltage gets lower and the discharge current gets larger. This can be verified from the electrical characteristics of a 50 kHz jet (Figure 2) and a 13.56 MHz jet (Figure 4). The influence of the gas flow rate on the behaviors of the electrical parameters of the plasma (voltage and current) is also shown in Figure 4a and b. For a fixed value of the input RF power, by increasing the gas flow rate, the plasma volume increases.[30] Thus, accepting that the ionization degree is almost constant, the plasma current increases while the applied voltage decreases. Figure 5a shows the variation of the total current with the applied voltage for the three different cases (one without the metal plane electrode and others with the plane electrode of distances $d = 3$ and 6 mm). Similar to the LF plasma jet, the case of small d has a higher current, and the increase rate of the current with the applied voltage is bigger than that of the LF jet. At a given applied voltage, the electric field increases with decreasing electrode gap (d) and causes an increase of the ionization rate in the plasma. Figure 5b shows the variation of the current collected at the ground plane electrode with the input RF power for two distances of the plane electrode from the pin ($d = 2$ and 4 mm). When a ground electrode was placed 5 mm away

DOI: 10.1002/ppap.200850001

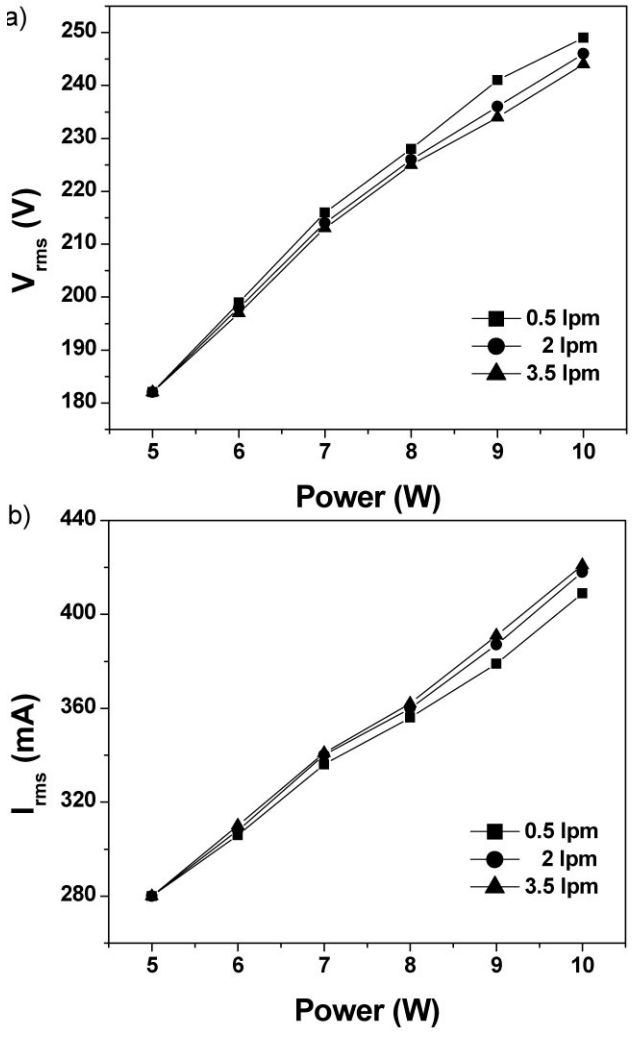

Figure 4. The voltage and total current as a function of input power for different flow rates.

from the Perspex tube, the plasma plume barely touched the ground electrode. By increasing the input power from 5 W to 9 W, the current through the ground plane electrode was increased from 21 mA_{rms} to 31 mA_{rms} for the distance of 4 mm. The increase rate of the current with the input power became large for the distance of 2 mm. It was observed that the plasma increased in brightness when the electrode gap (d) is decreased, and the glow expanded and spread over the surface.[10] The electron temperature (T_e) is estimated at about 0.2 eV from swarm parameters of electron in helium using the well-known Einstein's equation $k_B T_e/e = D_e/\mu_e$, where μ_e, k_B, and D_e are drift mobility, Boltzmann constant, and the diffusion constant. For the input RF power of 7 W and the electrode gap of 2 mm, the electron density (n_e) is about $2.5 \times 10^{12}\,cm^{-3}$ from the calculation based on the relation $n_e = J/(E\,\mu_e\,e)$, where J is the current density and E is the electric field.[4] Figure 5c shows the measured gas

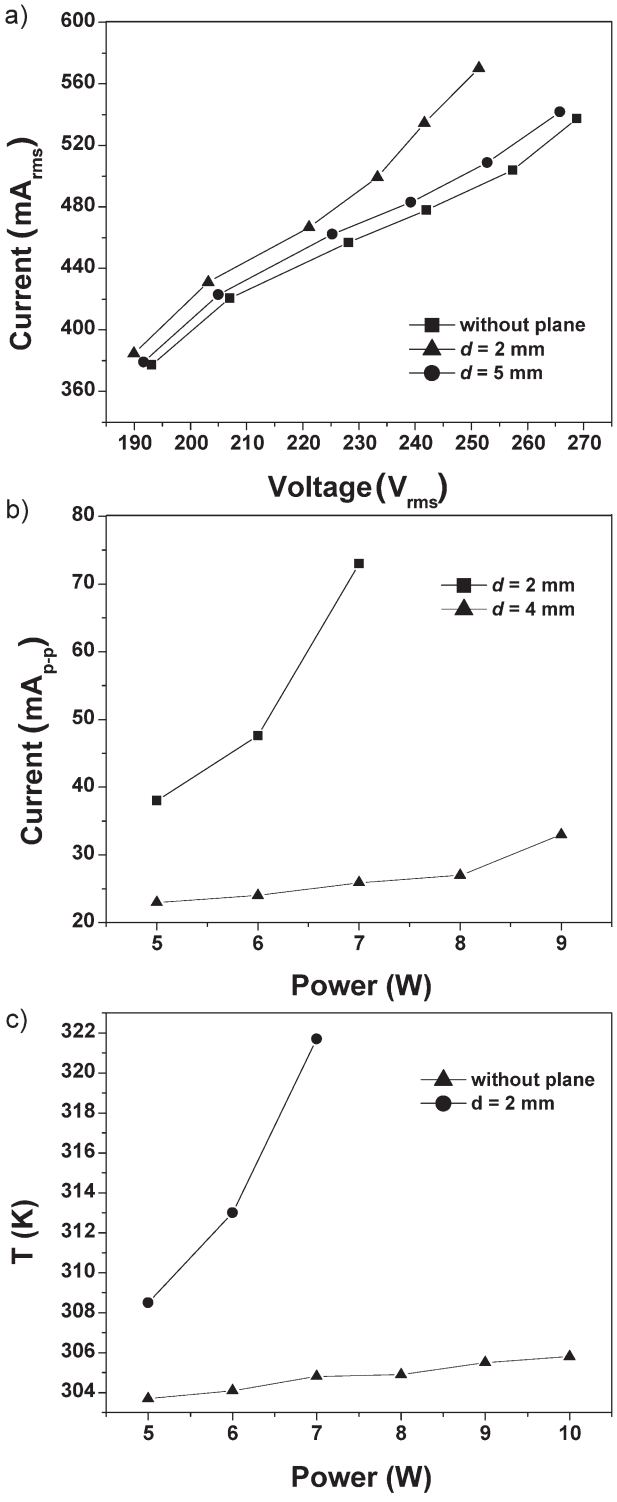

Figure 5. a) Total current as a function of applied voltage for the cases of no metal plane and of the plane with two different d at the frequency of 13.56 MHz and the gas flow rate of 0.5 $l \cdot min^{-1}$. b) The current collected at the ground plane electrode as a function of the input RF power for two distances of the plane electrode from the pin ($d = 2$ and 4 mm). c) The measured gas temperature as a function of input RF power.

temperature as a function of input power for RF plasma jets with and without a ground plane electrode. A continuous increase in the gas temperature can be seen as the RF power increases. An increase in the plasma power leads to an increase of the plasma volume, which is immediately reflected by the gas heating. With a ground plane electrode, the discharge has a larger gas temperature and the increase rate of gas temperature with input power becomes higher. Compared to Figure 2h, the gas temperature of the RF jet is higher than that of the LF jet and this is consistent with its stronger optical emission. The gas temperature (T_g) of the plasma can be deduced from the rotational temperature (T_r) of diatomic species, which is expected to be in equilibrium with T_g. The rotational temperature of a molecule can be obtained by comparing the synthetic diatomic molecular spectrum with measured one.[31] To obtain the best fit between the experimental and the synthetic spectral bands, a least-square procedure is used. A typical fitting of the measured band spectrum with the synthetic spectrum is shown in Figure 6a and b. The N_2^+ first negative system band from 390 nm and 392 nm for the 391.44 nm line of the measured first negative (0,0) band is fitted with the synthetic spectrum to obtain N_2^+ rotational temperature (Figure 6a). The OH band ($A\ ^2\sum^+ \rightarrow X\ ^2\Pi$ transition) from 306 nm and 310 nm is fitted to obtain OH rotational temperature in Figure 6b. Good agreement between the measured spectrum and the synthetic suggests reasonable evaluation of T_r. The rotational temperature compares well with the gas temperature for the RF plasma jets without a ground plane electrode in Figure 5c. Figure 7a shows the

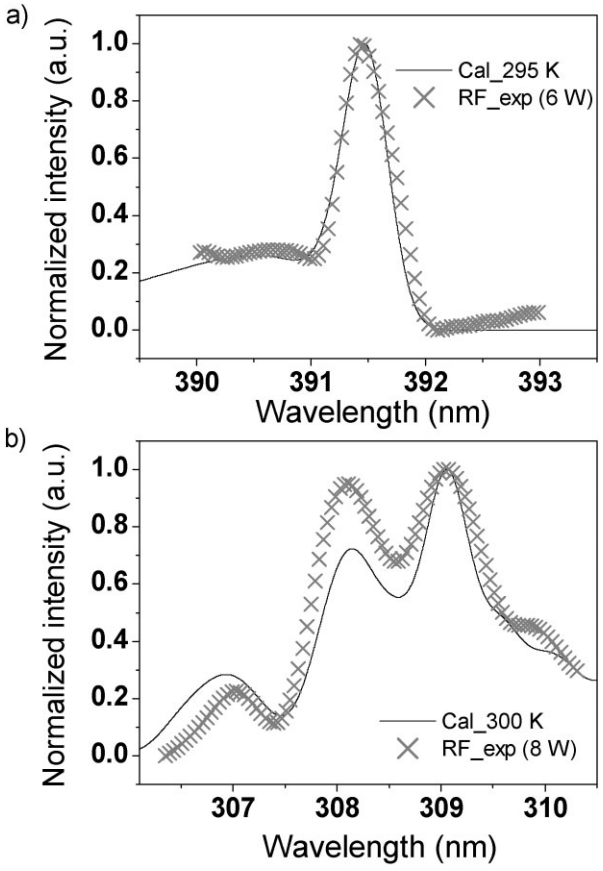

Figure 6. Comparison of experimental and simulated spectra of a) N_2^+ first negative system 0-0 transition. b) OH ($A\ ^2\sum^+ \rightarrow X\ ^2\Pi$, 306 - 310 nm) transition for T_r measurement of the RF jet.

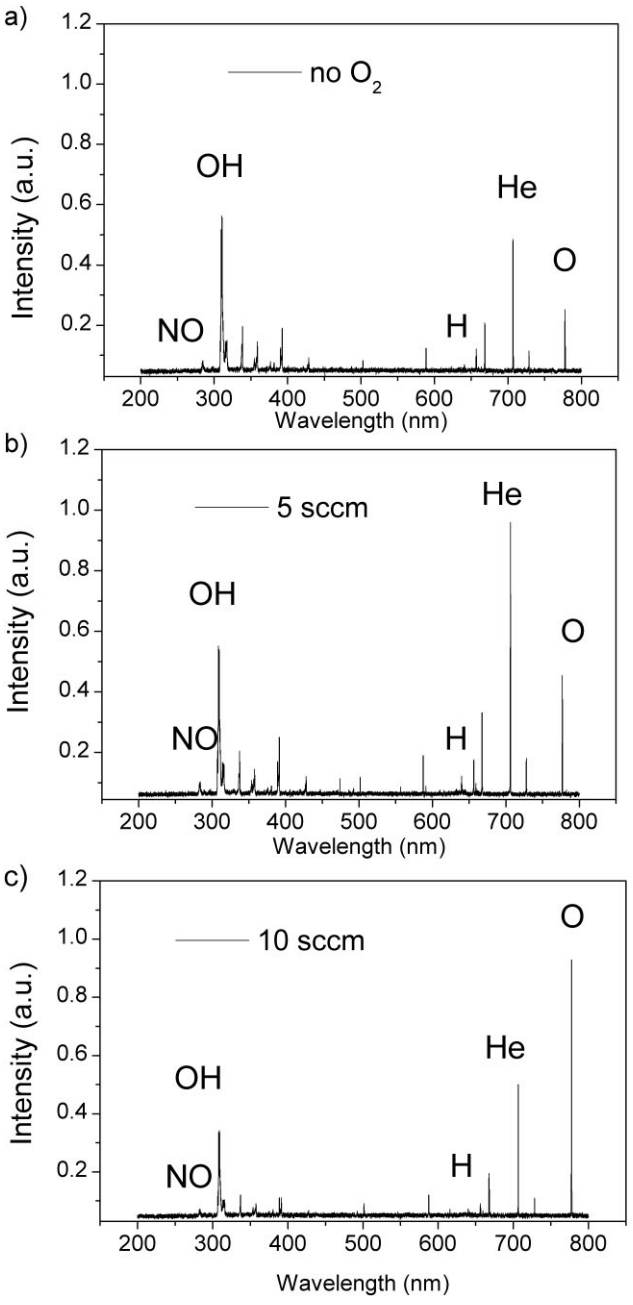

Figure 7. Emission spectrum from 200 nm to 800 nm observed in RF plasma jet (6 W, 1 l · min^{-1}) with different input gas. a) He only, b) He with the 5 sccm of oxygen gas, and c) He with the 10 sccm of oxygen gas.

Plasma Process. Polym. **2009**, *6*, 676–685

DOI: 10.1002/ppap.200850001

emission spectrum observed in the RF plasma jet (6 W, 1 l · min^{-1}). In the emission spectrum, we observed strong OH and weak N_2 molecular bands, as well as strong atomic lines of He and O. Compared with the LF plasma jet spectrum, the RF jet spectrum has much higher intensity in helium atomic lines indicating larger plasma density and/or electron temperatures.[7] The intensity from NO remains almost unchanged or slightly decreases. Another main difference between the LF and RF spectra relies on the relative intensity of the nitrogen band.[28] The strongest emission is the N_2^* line at 337.2 nm in the LF jet, whereas in the RF jet it is the OH line at 306 nm (the next stronger one is the excited He atom line at 706.5 nm), suggesting a difference in their electron energy distribution function. Since the critical radicals to cell death are just O and OH radicals, the richness of O, H, and OH species makes the RF microplasma jets more suitable for the biomedical applications.[13,32] Figure 7b and c show the emission spectra when oxygen gas is added into helium to generate more reactive species, which play a significant role in sterilization. As the oxygen flow rate increases, higher excited oxygen line is observed, while hydroxyl line is decreased slightly. At the oxygen flow rate of 10 sccm (which is equivalent to 1 volume percent in helium), the helium peak (at 706.5 nm) decreases, indicating that electrons dissipate more of their energy through collisions with oxygen molecules rather than with helium atoms.[33] The RF microplasma jets have higher plasma intensity and lower excitation voltage, but their power consumption and gas temperature are generally much higher. When an external loop wire is placed near the outlet of the glass tube serving as a ground electrode (instead of the plane electrode), it is observed that the plasma plume gets thicker and the discharge current increases and the optical emission intensities from the RF plasma plume are enhanced significantly indicating that the generated plasma is near the glow discharge mode.[25] Figure 8 shows the amplitude of the RF voltage as a function of the input RF power for the cases with and without the loop wire. In presence of the loop wire, the voltage is decreased and the current is increased. However, the plasma is disturbed significantly, and this limits the use of the loop wire for certain applications.

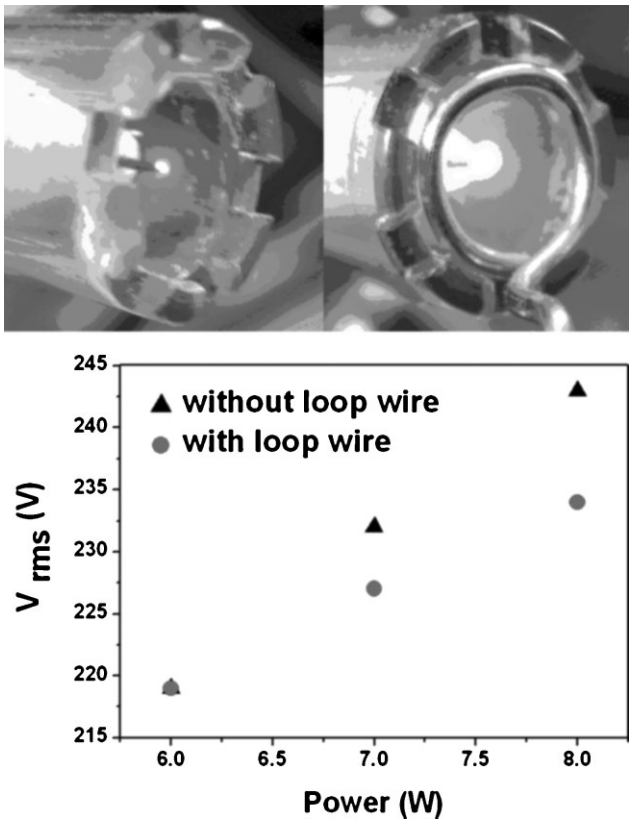

Figure 8. Voltage versus applied RF power for two operating conditions (with and without the loop wire). The photograph shows a plasma plume with loop wire.

Bacterial Inactivation

For the biomedical application of the plasma jets, the bacterial inactivation experiment using the two types of source (LF and RF) was performed. We did not explore the effects of every geometrical and operation parameters of the plasma jets on the bacterial inactivation. Instead, plasma power (or applied voltage), treatment time, and pin (needle)-to-sample distance were varied. The direct plasma treatment implies that living tissue itself is used as one of the electrodes and directly participates in the active plasma discharge process. Neither the plane ground electrode, nor the loop wire is used in the bacterial inactivation experiment. Figure 9a shows the survival curve of E. coli for different discharge conditions. Two cases of LF (50 kHz) jets (applied voltage 1 400 V and 1 700 V with distance 1.5 cm) and three cases of rf jets (input power 8 W with 5 mm distance, 10 W - 5 mm, and 8 W - 2 mm) are considered. The vertical axis is the log of the number of viable E. coli remaining (N) to the control number (N_0). The dotted lines represent fitting curves using the least-squares non-linear regression. Some cases show a clear pattern of multi-phase inactivation curves. In low pressure systems, one often observes fast initial sterilization efficiency, followed by a long tailing due to shadowing effects.[34] Even in atmospheric pressure systems, when samples are treated by large area dielectric barrier discharge sources or the plasma jets with higher power (or applied voltage), one may observe a similar trend.[15,16,35] However, in the treatment done by low-power plasma jets, the sterilization curve can be approximated as either straight line,[10,14] or as multi-phase nonlinear curve[11] in a log scale. The sterilization kinetics depends on both the type of the microorganisms and the

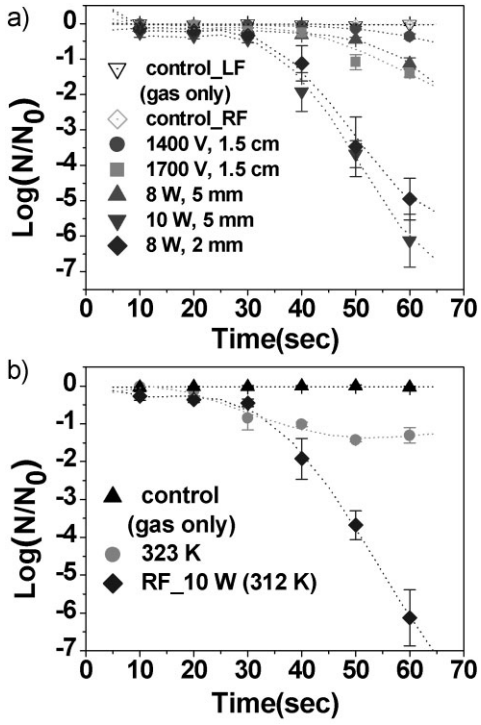

Figure 9. a) Survival curve of E. coli for different discharge conditions (the LF jets with 1400V and 1700 V (distance 1.5 cm), the RF jets with 8 W - distance 5 mm, 10 W - 5 mm, 8 W - 2 mm). b) Effect of hot plate temperature on the survival of E. coli (circle symbols) and the comparison with the plasma treatment.

characteristics of the plasma plume (which is determined by plasma gas, power coupling mechanism, and electrode geometry).[10,11,15,16,35] It should be also noted that the treatment time of 60 s is not sufficient to explore the sterilization kinetics of the microorganisms. The sterilization efficiency is proportional to the input power (or the applied voltage). Almost all E. coli were killed in about 60 s at 5 mm distance for the RF jet of 10 W. The increasing exposure distance reduces the sterilization efficiency by separating the sample from the energetic plasma source, and by reducing plasma activity by decreasing power.[10] The decimal reduction time (D value) for the RF plasma jet are 36 s (10 W, 5 mm, 1 $l \cdot min^{-1}$), 44 s (8 W, 2 mm, 1 $l \cdot min^{-1}$), and 58 s (8 W, 5 mm, 1 $l \cdot min^{-1}$). The D value for the LF plasma jet is 47 s (1700 V, 1.5 cm, 2 $l \cdot min^{-1}$). A reduction factor of about 6 logarithmic steps is achieved at 60 s in the RF jet of 10 W. The experimental data show that the sterilization efficiency of the RF plasma jet is generally better than that of LF plasma jet. However, LF plasma jet has an advantage when the plasma device needs to be at a substantial distance from the sample. Moreover, the situation can be changed when either higher voltage (e.g., 5–9 kV) LF or narrow high voltage pulses (with repetition rates in the kilohertz range) are used as excitation sources of the plasma jet. The current results indicate that the LF plasma jet with a little higher voltage than that employed in this work can achieve a level of sterilization efficiency comparable to that of the RF jet. It has also been known that that the addition of a small amount of O_2 gas to pure helium results in an efficient sterilization.[1,14] This study also confirmed this phenomenon, but a detailed analysis was given in a separate paper.[36] The E. coli is extremely sensitive to heat (for temperature above 40 °C). As can be seen in Figure 2h and Figure 5c, the gas temperatures of the LF jet and the RF jet are near room temperature. To explore the heat effect of sterilization, the substrate was heated to 323 K (above the gas temperature of 312 K for the RF jet of 10 W) using a hot plate (WiseStir MSH-20D), and the gas was flown. As can be seen in Figure 9b, the population of E. coli heated on the hot plate was decreased at the plate temperature of 323 K, until 35 s, and then the survival population was saturated. But, the RF plasma treatment corresponding to the same plume temperature resulted in a drastic reduction at 40 s. In the plasma treatment, since the distance between the tip and the sample is several millimeter, actually the plume temperature is not reached uniformly over the sample. Thus, the bacterial inactivation by plasma plume occurs locally, whereas the hot plate heats the sample uniformly. The inactivation efficiency of the RF plasma is significantly greater than that of hot gas only as the exposure time is increased above 35 s. UV radiation is important factor responsible for sterilization of E. coli when the exposure distance is short and the gas flow rate is small.[12,14] However, when liquid samples are treated as in this work, short-wavelength radiation is cut off by water. Therefore, the primary role in the inactivation is expected to be played by reactive species including oxygen, OH, H, and NO with minor aid from heat, UV photons, charged particles, and electric fields.[16,36] This is confirmed by the correlation of the survival curve with the optical emission spectra. If the sample is exposed by plasma with being placed on the plane electrode, the sterilization can be expedited due to a drastic increase in the gas temperature (see Figure 5c).

Conclusion

In summary, compact microplasma jet devices are developed at atmospheric pressure excited at a several tens of kilohertz and 13.56 MHz. With various geometrical and operational parameters changed, the plasma jets showed different discharge characteristics. As the length of the pin wire exposed to the plasma (p) is increased, the length of the plasma plume increases, but the current is decreased. The distance between the pin to the outlet of the glass tube (s) does not make significant effect on the total current. When a conducting material, an iron plane electrode, was placed

DOI: 10.1002/ppap.200850001

near the pin electrode, the electrical characteristics and gas temperature of the microplasma jets were changed. As the distance between the pin and the plane electrode (d) is decreased, the current through the metal plane increases and the increase rate of that current with the input power becomes higher. In presence of a plane electrode, the gas temperature tends to increase, and the increase rate of the gas temperature with input power becomes higher. The operational parameters include the applied voltage (amplitude and frequency) and the gas flow rate. The developed microplasma jets proved to be low current and low gas temperature. They are utilized to perform the bacterial inactivation experiments. The survival curves of E. coli are obtained for different discharge conditions. The experimental data show that the sterilization efficiency of the RF plasma jet is generally better than that of LF plasma jet. The primary role in the inactivation is expected to be played by reactive oxygen species with minor aid from UV photons, charged particles, heat, and electric fields. This point can be seen from the comparison of the optical emission spectra for the LF and RF jets. The richness of O and OH species in the plasma plume makes the RF microplasma jets more suitable for the biomedical applications. However, it is expected that the LF plasma jet implemented with proper parameters can achieve a level of sterilization efficiency comparable to that of the RF jet.

Acknowledgements: This work was supported by the *Korea Science and Engineering Foundation* under Contract No. 2008-01011. Helpful discussions with Dr. *C. H. Shon* of *Korea Electrotechnology Research Institute*, Professor *J. K. Lee* of *Pohang University of Science and Technology*, and Professor *W. Choe* and Dr. *S. Y. Moon* of *Korea Academic Institute of Science and Technology* are greatly acknowledged.

Received: January 12, 2009; Revised: June 10, 2009; Accepted: June 18, 2009; DOI: 10.1002/ppap.200850001

Keywords: atmospheric pressure microplasma jets; bacterial inactivation; cold plasma sources; non-thermal plasmas

[1] M. Laroussi, T. Akan, *Plasma Process. Polym.* **2007**, *4*, 777.
[2] C. Oliveira, J. A. Souza Corrêa, M. P. Gomes, B. N. Sismanoglu, J. Amorim, *Appl. Phys. Lett.* **2008**, *93*, 041503.
[3] X. Zhang, M. Li, R. Zhou, K. Feng, S. Yang, *Appl. Phys. Lett.* **2008**, *93*, 021502.
[4] T. L. Ni, F. Ding, X. D. Zhu, X. H. Wen, H. Y. Zhou, *Appl. Phys. Lett.* **2008**, *92*, 241503.
[5] X. P. Lu, Z. H. Jiang, Q. Xiong, Z. Y. Tang, X. W. Hu, Y. Pan, *Appl. Phys. Lett.* **2008**, *92*, 081502.
[6] I. E. Kieft, E. P. van der Laan, E. Stoffels, *New J. Phys.* **2004**, *6*, 149.
[7] D. B. Kim, J. K. Rhee, B. Gweon, S. Y. Moon, W. Choe, *Appl. Phys. Lett.* **2007**, *91*, 151502.
[8] N. Puac, Z. L. J. Petrovic, G. Malovic, A. Dordevic, S. Zivkovic, Z. Giba, D. Grubisic, *J. Phys. D: Appl. Phys.* **2006**, *39*, 3514.
[9] G. Li, H.-P. Li, L.-Y. Wang, S. Wang, H.-X. Zhao, W.-T. Sun, X.-H. Xing, C.-Y. Bao, *Appl. Phys. Lett.* **2008**, *92*, 221504.
[10] E. Raymond, R. J. Sladek, E. Stoffels, R. Walraven, P. J. A. Tielbeek, R. A. Koolhoven, *IEEE Trans. Plasma Sci.* **2004**, *32*, 1540.
[11] S. Perni, G. Shama, J. L. Hobman, P. A. Lund, C. J. Kershaw, G. A. Hidalgo-Arroyo, C. W. Penn, X. T. Deng, J. L. Walsh, M. G. Kong, *Appl. Phys. Lett.* **2007**, *90*, 073902.
[12] T. Sato, T. Miyahara, A. Doi, S. Ochiai, T. Urayama, T. Nakatani, *Appl. Phys. Lett.* **2006**, *89*, 073902.
[13] J. F. Kolb, A. A. H. Mohamed, R. O. Price, R. J. Swanson, A. Bowman, R. L. Chiavarini, M. Stacey, K. H. Schoenbach, *Appl. Phys. Lett.* **2008**, *92*, 241501.
[14] H. S. Uhm, J. P. Lim, S. Z. Li, *Appl. Phys. Lett.* **2007**, *90*, 261501.
[15] X. T. Deng, J. J. Shi, G. Shama, M. G. Kong, *Appl. Phys. Lett.* **2005**, *87*, 153901.
[16] H. W. Herrmann, I. Henins, J. Park, G. S. Selwyn, *Phys. Plasmas* **1999**, *6*, 2284.
[17] X. T. Deng, J. J. Shi, M. G. Kong, *J. Appl. Phys.* **2007**, *101*, 074701.
[18] X. T. Deng, J. J. Shi, H. L. Chen, M. G. Kong, *Appl. Phys. Lett.* **2007**, *90*, 013903.
[19] S. Forster, C. Mohr, W. Viol, *Surf. Coat. Technol.* **2005**, *200*, 827.
[20] M. Teschke, J. Kedzierski, E. G. Finantu-Dinu, D. Korzec, J. Engemann, *IEEE Trans. Plasma Sci.* **2005**, *33*, 310.
[21] A. Fridman, A. Chirokov, A. Gutsol, *J. Phys. D: Appl. Phys.* **2005**, *38*, R1.
[22] X. T. Deng, M. G. Kong, *IEEE Trans Plasma Sci.* **2004**, *32*, 1709.
[23] A. Schutze, J. Y. Jeong, S. E. Babayan, J. Park, G. S. Selwyn, R. F. Hicks, *IEEE Trans. Plasma Sci.* **1998**, *26*, 1685.
[24] D. B. Kim, J. K. Rhee, S. Y. Moon, W. Choe, *Appl. Phys. Lett.* **2006**, *89*, 061502.
[25] X. P. Lu, Z. H. Jiang, Q. Xiong, Z. Y. Tang, Y. Pan, *Appl. Phys. Lett.* **2008**, *92*, 151504.
[26] J. L. Walsh, J. J. Shi, M. G. Kong, *Appl. Phys. Lett.* **2006**, *88*, 171501.
[27] M. Laroussi, X. Lu, *Appl. Phys. Lett.* **2005**, *87*, 113902.
[28] M. H. Guerra-Mutis, C. V. Pelaez U, R. Cabanzo H, *Plasma Sources Sci. Technol.* **2003**, *12*, 165.
[29] G. Fridman, A. Shereshevsky, M. M. Jost, A. D. Brooks, A. Fridman, A. Gutsol, V. Vasilets, G. Friedman, *Plasma Chem. Plasma Process.* **2007**, *27*, 163.
[30] S. D. Anghel, A. Simon, *Meas. Sci. Technol.* **2007**, *18*, 2642.
[31] S. Y. Moon, W. Choe, *Spectrochim. Acta, Part B* **2003**, *58*, 249.
[32] J. Goree, B. Liu, D. Drake, E. Stoffels, *IEEE Trans. Plasma Sci.* **2006**, *34*, 1317.
[33] G. Park, H. Lee, G. Kim, J. K. Lee, *Plasma Process. Polym.* **2008**, *5*, 569.
[34] S. Hury, D. R. Vidal, F. Desor, J. Pelletier, T. Lagarde, *Lett. Appl. Microbiol.* **1998**, *26*, 417.
[35] K.-D. Weltmann, R. Brandenburg, T. von Woedtke, J. Ehlbeck, R. Foest, M. Stieber, E. Kindel, *J. Phys. D: Appl. Phys.* **2008**, *41*, 194008.
[36] S. J. Kim, T. H. Chung, S. H. Bae, S. H. Leem, *Appl. Phys. Lett.* **2009**, *94*, 141502.